Earth Systems and Environment (2020) 4:167–181
https://doi.org/10.1007/s41748-019-00143-8

ORIGINAL ARTICLE

Spatial and Temporal Variations of Erosion and Accretion: A Case of a Large Tropical River

Ashty Saleem[1] · Ashraf Dewan[1] · Md Masudur Rahman[2] · Shahrin M. Nawfee[3] · Rajimul Karim[4] · Xi Xi Lu[5]

Received: 29 July 2019 / Accepted: 7 December 2019 / Published online: 21 December 2019

Abstract

Rapidly changing river systems can impact people, property and infrastructures. This study investigates bank erosion and accretion of the Padma River in Bangladesh, through space and time, using historical topographic maps, Corona and Landsat images and navigational charts. A geographic information system (GIS) was utilised to quantify the erosion and accretion pattern. In addition, volumetric changes in the riverbed were also investigated. Results indicated that the area of erosion and deposition vary both spatially and temporally. However, erosion was more prominent on the left bank, whilst accretion was high along the right bank, over the study period. Overall, average annual erosion rates were higher than accretion rates (17 km^2 $year^{-1}$ versus 13 km^2 $year^{-1}$). The volumes of morphological change for two epochs correspond to a net volume gain of 338.75 million m^3 sediment between 1984 and 1992 but a net loss of 295.20 million m^3 during the period 1992–2008. Regression analysis between bank erosion and mean annual flow, peak discharge and mean flood flow showed that two of the three independent variables were significantly associated with bank erosion. The area of large mid-channel bars increased over time, which may have had a role in shaping erosion and accretion processes of the river. As increased runoff is expected in the future, as a result of enhanced rainfall under warmer climate, knowledge of this work will help to determine the morphological response of fluvial systems in Bangladesh and elsewhere.

Keywords Padma river · Erosion · Accretion · Bathymetry · Morphological change

1 Introduction

River bank erosion and accretion (deposition) are the two key geomorphic processes of a fluvial system. Bank erosion is detrimental to riparian areas and has various geomorphic, social and economic consequences (Wang et al. 2016), whereas accretion can reduce conveyance capacity (Bizzi and Lerner 2015), making navigation potentially more difficult. Though both processes are common in the deltaic plains of South Asia, severe erosion is identified as one of the major causes of arable land loss and population displacement (Thakur et al. 2012). As studies of global change require a deeper understanding of geomorphic change

Electronic supplementary material The online version of this article (https://doi.org/10.1007/s41748-019-00143-8) contains supplementary material, which is available to authorized users.

✉ Ashty Saleem
ashty.saleem@curtin.edu.au

Ashraf Dewan
a.dewan@curtin.edu.au

Md Masudur Rahman
masud_ra0171@yahoo.com

Shahrin M. Nawfee
smnawfee@gmail.com

Rajimul Karim
razimulseye@gmail.com

Xi Xi Lu
geoluxx@nus.edu.sg

[1] Curtin University, School of Earth and Planetary Sciences, Perth, WA 6102, Australia

[2] Department of Geography and Environment, University of Dhaka, Dhaka 1000, Bangladesh

[3] Department of Environmental Management, Independent University, Dhaka 1229, Bangladesh

[4] Center for Geographic Information Services, Dhaka 1000, Bangladesh

[5] Department of Geography, National University of Singapore, 10 Kent Ridge Crescent, Singapore 119260, Singapore

(James et al. 2012), historical investigation of channel dynamics can provide spatial and temporal insights into the locations of bank movement and in understanding a channel's sensitivity to environmental conditions (Bizzi and Lerner 2015). Knowledge of the nature, rates and causes of channel change has considerable implications for minimizing flood risk (Tiegs and Pohl 2005), conserving biodiversity (Joeckel and Henebry 2008) and providing the basis for predicting the future evolution of a river (Shields et al. 2000; Surian 1999).

Although the rivers have been a lifeline for millions of people for millennia, frequent bank migration, resulting from natural factor such as floods and anthropogenic activities (e.g., land use change), is one of the causes of substantial land loss and property damages in Bangladesh (CDMP, 2014). For example, BBS (2016) estimated that a total of 428.7 km^2 of lands were lost to river/coastal erosion between 2009 and 2014, resulting in the loss of 36,409 m Taka (1 US$ ~ 78 BD Taka). In contrast, IWFM (2010) estimated that only 193 km^2 of lands were accreted by the major rivers during the preceding 10 years. As water-related hazards, resulting from increased river flow, such as bank erosion, are expected to increase in the Ganges–Brahmaputra system (Ikeuchi et al. 2015), knowledge of space–time variation of morphological change is valuable in supporting and building the adaptive capacity of the country to climate change.

A number of studies have been conducted, using both geospatial and, stratigraphic records and observed cross-section data, to assess channel dynamics of the Ganges (in the upper reach from the Indo–Bangladesh border to Aricha) (Dewan et al. 2017; CEGIS 2003) and the Brahmaputra (Sarker et al. 2014; Baki and Gan 2012). Compared with these works, relatively little is known about the planform behaviour and morphological response of floods of the Padma River. Though Dewan et al. (2017) provide some insights on its channel pattern, their study covered a relatively short-term period (38 years), and from the viewpoint of regulated versus unregulated rivers. Since short-term statistics are scattered (Wang et al. 2016) and may not necessarily represent long-term erosion and accretion trends, the use of records from further back (i.e. 100 years) may contribute to greater certainty (Scorpio and Rosskopf 2016), and more accurately delineate the stable and unstable reaches of a fluvial system (Winterbottom 2000). In addition, their work did not include bathymetric information for determining the volume of morphological change of the Padma. As time-series sediment data are very sparse for major rivers in Bangladesh, this study draws information from historical maps, satellite images and bathymetric records which could shed light on understanding reach-to-reach channel variability, caused by the erosion–accretion processes (Li et al. 2007). We, therefore, aimed to: (1) analyse patterns of erosion and accretion of the Padma system over a 100-year timespan; (2) quantify river islands and riverbed elevation changes; and (3) explore the role of floods in accounting for bank erosion.

2 Materials and methods

2.1 Study area

This study was conducted on a 112-km reach of the river Padma in Bangladesh (Fig. 1). It is a relatively young river that formed approximately 200 years ago (FAP 4 1993). Initially, it maintained its course through the Ganges along the Arial Khan River but, during a major avulsion between 1830 and 1857, it broke through the Chandina Alluvium to join the Meghna near Chandpur (FAP 16 1995). The total catchment area of the river is 1.7 million km^2, and includes the combined catchments of the Ganges and Brahmaputra (Nippon Koei Co. Ltd. 2005). It is a highly dynamic system, subject to erratic bank line shifting due to its annual high sediment load of about one billion metric tonnes (FAP 4 1993). The discharge of the river ranges from 4800 to 30,000 m^3 s^{-1} with a substantial bankfull flow of about 72,500 m^3 s^{-1}, making it the fourth largest river in the world in terms of flow (FAP 24 1996). The annual hydrograph of the river is characterised by low flows during the winter and high flows during monsoon, and the water level differences in a year are found to be 5-6 m (Nippon Koei Co. Ltd. 2005). Peak discharges during the floods of 1987, 1988, 1998 and 2004 were 118,000, 87,300, 116,011 and 103,358 m^3 s^{-1}, respectively.

2.2 Data acquisition and preparation

This study uses topographic maps, digital elevation models and multi-temporal remotely sensed data (Table 1). In addition, 4-week fieldwork was carried out in study area in 2015 to determine the location of the river boundary in support of bank delineation of 2015. Twenty sites, extending throughout the reach, were visited, and the number and location of bank failures, floodplain characteristics, bank protection types, and the exposure of land to flooding were recorded, as well as sampling of mid-channel bars. Further, three focus group discussions (FGD) and five key informant interviews (KII) were conducted to understand social issues and damage to property.

Fourteen navigational charts were collected from the Bangladesh Inland Water Transport Authority (BIWTA) to examine morphological processes. In addition, sixteen topographic maps (1:50,000), comprising the first (1960s) and fifth editions (2010s) were obtained from Survey of Bangladesh (SOB).

Long-term daily flow data for two gauge stations on the Padma were collected from the Bangladesh Water

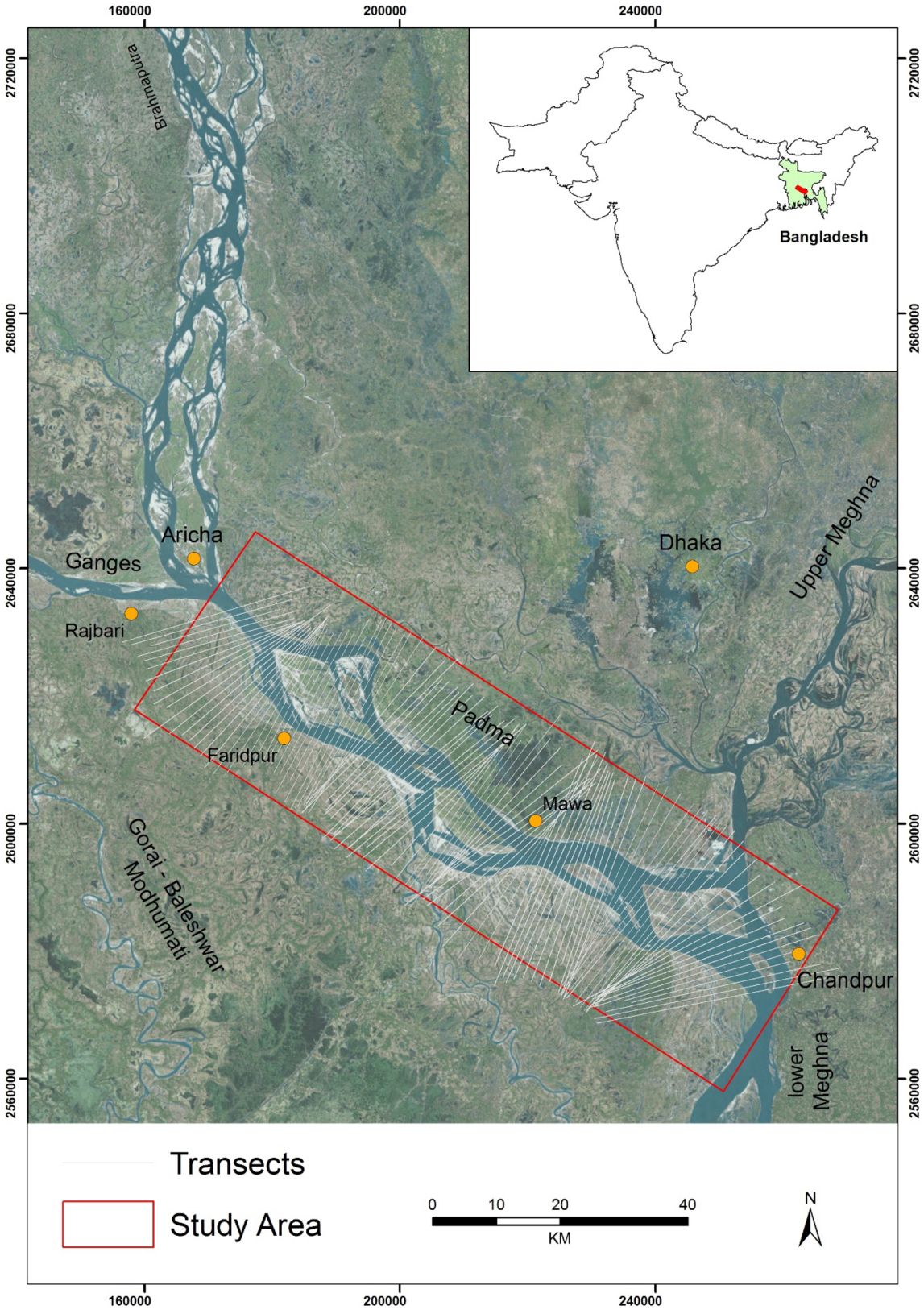

Fig. 1 Location of study area

Table 1 Source, types and scales/resolution of data used in this study

Type of data	Sources	Scale/resolution	Year
Topographic maps	British Library, University of Texas	1: 253,440	1911, 1930, 1944, 1955
Topographic maps	Survey of Bangladesh	1:50,000	First (1960s) and Fifth (2010s) editions
Corona photographs	USGS	10 m	1967
Landsat MSS	USGS	79 m	1977, 1984
Landsat TM	USGS	28.5 m	1995, 2005
Landsat 8	USGS	28.5 m	2015
Navigational charts	BIWTA	1: 50,000 and 1:25,000	1984, 1992, 2008
Water level/discharge	BWDB	Daily/monthly	1965–2014

Development Board (BWDB). These stations are Baruria (Station ID: SW91.9L) and Mawa (Station ID: SW93.5L). Since 1987, the Mawa station included only monsoonal (June–Oct) flow data.

2.3 Analytical techniques

Historical topographic maps were georeferenced and likewise, all navigational charts were rectified. Five Corona photographs and 10 cloud-free Landsat scenes were then georeferenced to the topographic maps which resulted in a Root Mean Square Error of < 0.5 pixels. Using the nearest neighbour technique, the images were resampled to 30-m pixel. Upon rectification, Corona and Landsat scenes were used to form an individual mosaic image for a year. Radiometric corrections of Landsat images included an image-based approach (Chavez 1996) to minimize the effect of changes in reflectance as well as varying sun angles. An area of interest (AOI) file, derived from a vector dataset, was subsequently utilised to clip individual datasets to the study area.

Visual interpretation of the river boundary from topographic maps and Corona data was undertaken assuming that the water surface depicted on the maps and photographs delineated the channel; however, this was not possible with Landsat data. Because of varying water levels and the presence of narrow and shallow channels, separation of land/water boundary from Landsat was a challenging task. To overcome this difficulty, a combination of Landsat bands (1–6–7) (Yang et al. 1999) and a soil–vegetation limit approach (Gurnell 1997) was employed to identify the river boundary. Previous studies (Winterbottom 2000; Yang et al. 1999) suggest that these approaches are effective to distinguish river planform, resulting from varying water levels within a channel. A single operator digitised the channel boundary, sandbars, and in-channel islands on screen at a scale of 1:5000 to maintain methodological consistency and precision. Spot heights (typical spacing between survey points, on average, is 150 m), and contours from navigation charts, representing active channel (e.g., both deep and shallow waters), were encoded using the same procedure but no side bar was taken into account. We then divided the 112 km of the river into 1-km profiles/transects ("profile" and "transect" are used interchangeably here) (Fig. 1). The profiles were developed perpendicular to the channel midline.

To estimate erosion and accretion patterns of the both banks, a new polygon was initially produced by taking the spatial union of two successive river polygons (e.g. 1911 and 1930) of a transect. The definition of each epoch is provided in Table S1. A negative value was assigned to denote erosion, indicating expansion of channel towards land. On the other hand, a positive value was used to characterise accretion, if a polygon decreased, i.e. retraction into the river. In case of no change between two dates, we assigned a zero value. This procedure was utilised for all segments in one epoch, and then repeated for each subsequent period. Note that we estimated total eroded and accreted areas for the entire channel as well as for the two banks separately, when determining both the spatial and temporal variations. To calculate annual rates of bank erosion and accretion for each epoch, the number of years in the epoch was considered.

To investigate channel topography, we constructed digital elevation model (DEM) of the riverbed using the inverse distance weighted method for 3 years (1984, 1992 and 2008) which were used to compute changes in volumes (Lane et al. 2003). Sandbars within the channel were masked out since they do not have elevation value attached. Average of lowest low water level (LLW) figure was used to derive riverbed topography. Two types of analyses were conducted. One involved the determination of net loss and gain to the riverbed through cut and fill analysis. In addition, cross-sectional change of the riverbed was examined using the same 1-km profiles. This was done by converting each transect to a point shape with a 50-m interval, so that detailed bathymetric change could be mapped.

In addition, morphological changes to islands in the river were calculated using their areas, shapes and sizes for different years. Total channel area for each period, including the area

occupied by mid channel bars, was calculated. The width of a river was defined as being the distance between the extreme right and left banks, which included the width of any mid-channel bars. The mean channel width for each reach was then computed from the sum of the appropriate widths. The ratio of island to channel area was analysed using both channel area and the sum of bar areas in an epoch.

Historical daily water level records were used to determine flood danger level (DL) (established by BWDB based on ground elevation of an area). This was then used to obtain corresponding discharge. This procedure helped us to define the Peak Over Threshold (POT) for Mawa station on the river. Based on the POT, flood frequencies and magnitudes were derived. Only valid data for each epoch for Mawa station were used for this purpose. Consideration was made for the fact that the geospatial data were representative of normal flow for the respective year, whilst floods take place in the earlier/later part of the year. Since the DL information for Baruria station was not available, the POT for this station was not attempted. However, mean annual flow for Baruria and Mawa stations was computed using monthly discharge data. Mean flood discharge for Mawa was obtained by dividing monsoonal flow (July–October) by the number of years of each interval. To understand the relative contribution of floods and water flow to bank erosion, linear regression between variables was performed.

To evaluate any propagation of errors or any uncertainty associated with morphological assessment, we adapted a method suggested by Yao et al. (2011). There were two main assumptions for this analysis. First, allowable systematic error (i.e. the georeferencing component), or the offset (dr), is approximately half of a pixel and uniform across the datasets; and secondly, the precision of feature identification (i.e. random error) is about 0.5 mm and invariant for both banks. Yao et al. (2011) noted that positional accuracy is influenced by area (S), perimeter (L) of a patch, and resolution of data (dr). A fishnet tool in a GIS was used to derive these parameters. The offset (dr) was multiplied by the perimeter to obtain the absolute area error (ds). The relative area error was then calculated by dividing the ds by the area of a patch. This method was applied for both banks separately. To quantify the vertical accuracy of riverbed elevations, the 95th-percentile technique was utilised, involving the construction of training and test datasets from the original elevation datasets (Bennion 2009). For each year, 10% of data from the original were randomly sampled and used as test points. The RMSE was then computed to provide a single error statistic for each year (FGDC 1998).

3 Results

3.1 Planform configuration

Successive channel planform maps are shown in Fig. 2, which demonstrates that the river experienced contraction and expansion as well as shape adjustments to its planform. Channel widening, for instance, was prominent during the first epoch (1911–1930), when the channel appeared to encroach onto the floodplains through lateral migration. Between 1944 and 1955, however, a small amount of channel contraction occurred due to deposition within its active corridor. Except for the epoch of 1977–1984, channel widening was pronounced but with varying rates (Fig. 2).

3.2 Riverbank shifting

Figure 3a highlights locational distribution of erosion and accretion areas along the left bank. For example, the erosion tendency of 19–46 km is relatively high, but is reduced between 49 and 63 km, and then increased downstream from 73 km until the confluence with the Meghna at Chandpur (Fig. 3a). The most unstable area, in terms of maximum erosion, is located between 96 and 111 km, where the erosion rate can be as high as 44 km^2 (100 km). Conversely, accretion was low between 6 and 25 km, and slightly increased from 26 to 32 km, 37 to 46 km and from 90 to 101 km.

The right bank of the river appears to be highly variable compared to the left bank (Fig. 3b). Interestingly, neither of the processes can be attributed to a specific direction. Bank erosion appears to be concentrated between 13 and 99 km which systematically increases from 103 to 112 km. In contrast, accretion occurs within the first few profiles (1–22 km) and then decreases slightly between 26 and 41 km.

Areas of erosion for both banks are shown in Table 2, which show that the right bank eroded more than the left bank of the Padma. With the exception of the first (1911–1930) and last (2005–2015) epochs, erosion was consistently higher along the right bank than the left bank. An estimated total 1749 km^2 of lands were eroded from 1911 to 2015 of which 807 km^2 were on the left bank, whilst 942 km^2 were on the right bank. The annual average bank erosion rate over the study period (1911–2015) was about 17 km^2 $year^{-1}$. Out of the 112 polygons, 35 on the left bank and 41 on the right bank experienced varying degrees of erosion during 1911–2015 (Table S2).

Table 3 presents the areas of accretion for both banks during nine epochs. It shows that a total of 1316 km^2

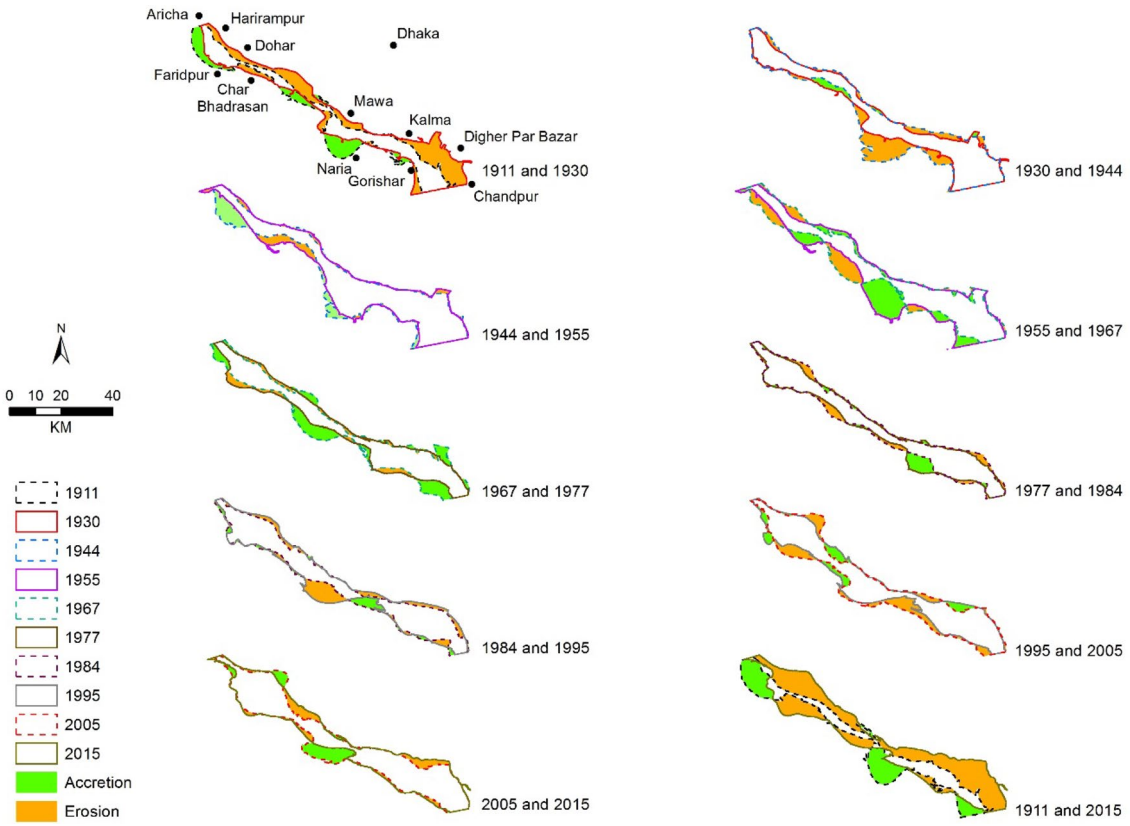

Fig. 2 Spatial distribution of bank erosion and accretion along the study reach, between 1911 and 2015, showing epochal changes in channel location. Channel at start of epoch shown as hollow; at end of epoch with solid fill

lands were accreted, of which the contribution of the right bank was 1062 km^2 and the left bank was 254 km^2. Interestingly, the right bank accreted higher amounts than the left bank, even though the right bank erodes highly (Table 2). The annual average accretion rate was approximately 13 km^2 year^{-1} from 1911 to 2015. The distribution of bank accretion figures is shown in Table S3.

FGDs and KII demonstrated that bank erosion is leading to a number of social issues, including loss of property and livelihood, particularly to marginalised groups. We interviewed a number of people who experienced bank erosion more than six times at Mawa and further downstream. This phenomenon frequently forcing them to move away, and property loss over three–four generations was substantial. In addition, a number of business centres, many buildings, both private and public, either had to relocate or washed away due to the devouring effect of the river. Local people assert that increasing river training works linked with construction of the Padma Bridge may be accountable for gobbling of properties and lands, particularly in recent times.

3.3 Changes in riverbed elevation

Riverbed elevation models along with corresponding longitudinal profiles for 3 years are shown in Fig. 4, which indicates that the range of elevations in 1992 (− 27 to 8 m) was generally higher than in 1984 (− 35 to 3 m). In contrast, bottom elevations decreased from 1992 to 2008 (from − 30 to 2 m). The cut and fill analysis indicates that the Padma gained a net volume of 338,752,966 (339 m) m^3 of sediment between 1984 and 1992 with an average of 42 m m^3/year over the 8 years; however, in the latter period, the river lost a volume of 295,196,067 (295 m) m^3 with an average of 18 m m^3 sediment per year (Table 4). Note that this calculation was heavily impacted by the lack of common surfaces between survey years (63.7% areas were common during 1984–1992 and 61.3% in 1992–2008), and therefore, may have estimation errors attached.

Of the 112 transects analysed, a few representative ones were sampled, covering upper, middle and lower reaches of the river (Fig. 5a–c). A typical profile (transect # 4 centred at 89.82 E and 23.76 N), covering the upper reach, is shown in

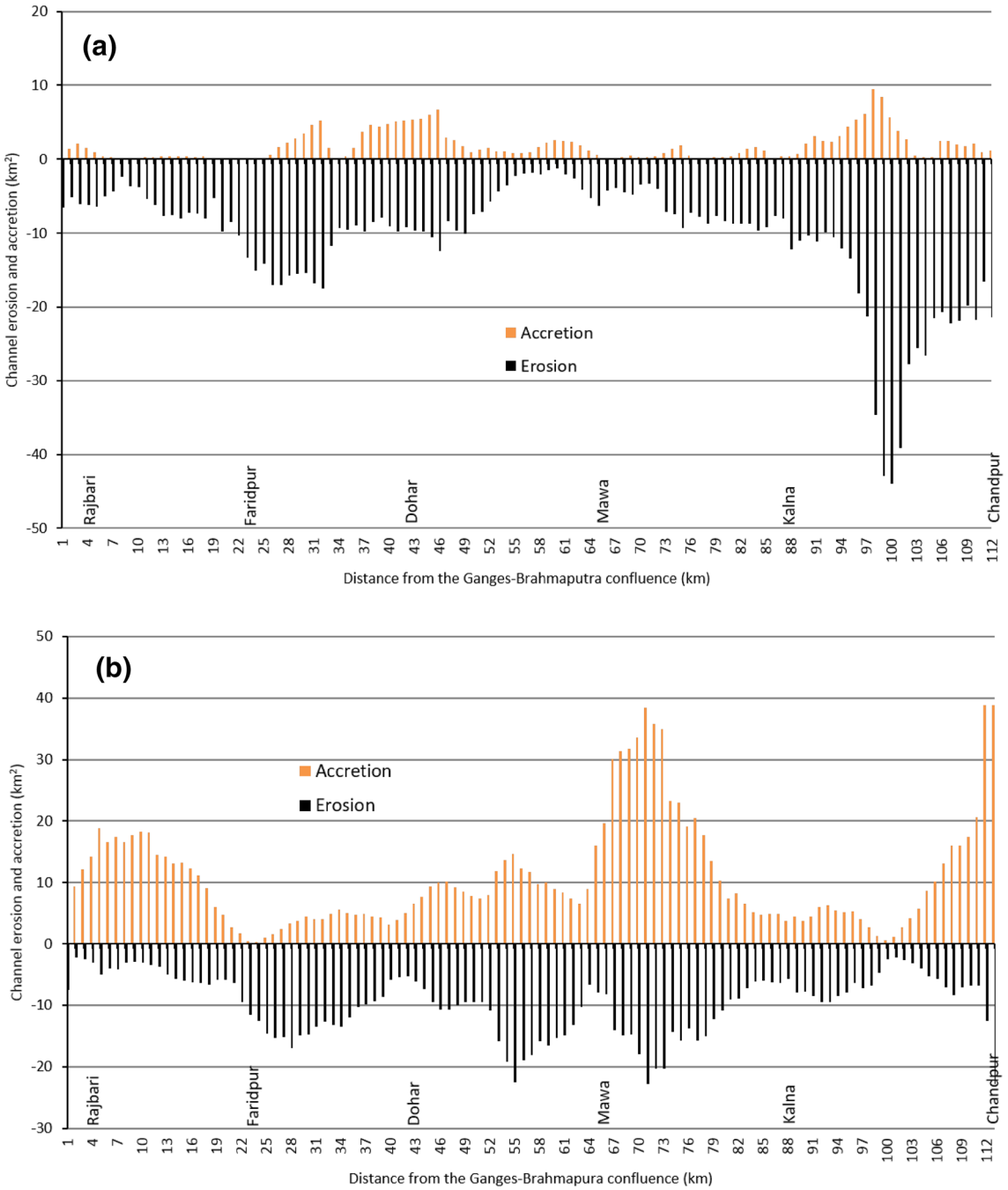

Fig. 3 Distribution of erosion and accretion, 1911–2015; **a** left bank; **b** right bank. Separate analysis is carried out for the left and right banks of the river

Fig. 5a. This indicates that the deepest channel in 1984 was around the mid-point of the river but shifted towards the left bank in 1992. During 1992–2008, both banks experienced substantial siltation, which resulted in a further change in thalweg position. The movement of the thalweg is highly erratic at transect # 49 (90.29E and 23.43N), representing the middle reach, between survey dates (Fig. 5b). For instance, the deepest point was located around the mid-point of the channel in 1984, but moved 1.9 km towards the right bank by 1992, then shifted again towards the left bank by about 3.5 km during 1992–2008, due to channel shrinkage in 2008. The last transect (ID = 112, 90.48E and 23.36N) (Fig. 5c) was located near the confluence of the Padma and Meghna, and indicates that the roughness of the riverbed was higher than the other transects across 3 years analysed but that both banks experienced erosion and accretion. The

Table 2 Areas of bank erosion along the right and left banks of the Padma, 1911–2015

Epochs	Area of erosion (km^2)		
	Left Bank	Right Bank	Total
1911–1930	317	62	379
1930–1944	76	219	294
1944–1955	37	75	112
1955–1967	44	152	196
1967–1977	40	61	101
1977–1984	56	62	119
1984–1995	79	118	197
1995–2005	58	149	207
2005–2015	98	44	142
Total (1911–2015)	807	942	1749

Table 3 Areas of bank accretion along the right and left banks of the Padma, 1911–2015

Epochs	Area of accretion (km^2)		
	Left bank	Right bank	Total
1911–1930	5	175	180
1930–1944	13	33	47
1944–1955	12	142	154
1955–1967	49	255	304
1967–1977	65	174	240
1977–1984	16	68	84
1984–1995	5	64	69
1995–2005	60	50	110
2005–2015	28	101	129
Total (1911–2015)	254	1062	1316

deepest point moved about 2.6 m to the right and the right bank accreted more than the left bank from 1984 to 1992. Between 1992 and 2008, erosion along the left bank was high, as was the level of scouring.

Changes in mean elevation, between years, for each profile, can be found in Fig. 6. The magnitude of change for the entire channel was approximately 7 m during 1992–2008 and riverbed erosion was higher in this period compared with 1984–1992, reflecting roughness of the riverbed. There are certain locations where elevation change occurred in an opposite fashion during the two periods studied. For instance, at 22–34 km, mean elevation decreased in 1984–1992 but reversed during 1992–2008.

3.4 Growth of bars and islands

Statistics on the growth of islands and their areas are shown in Table 5, which indicates that the number of islands (sum of vegetated islands and sandbars) was a maximum in 1967; however, this may be related to the resolution of Corona data. The relationship between the mean river width and areas of mid-channel bars over time was found to be positively correlated ($r^2 = 0.62$) (Fig. 7). The ratio of island area to channel area, although varied between 1911 and 1984, has generally increased since 1911 (Table 5). Interestingly, this variability has strong similarities to the fluctuations of the river width. Figure 8 shows that islands having an area of ≥ 5 km^2 increased consistently since 1977, indicating that the river was dominated by the growth and accretion of large islands.

3.5 Role of floods on bank erosion

Analysis of the role of flood discharge (July–October) on the annual rate of erosion and accretion is shown in Table 6. This indicates that flood has had a significant role in the erosion–accretion processes. For example, except for the epoch of 1967–1977, bank erosion tended to increase as discharge went up. However, an opposite relationship was observed for the annual accretion rate and peak flood discharge.

The relationship between annual peak flow and mean flood discharge at Mawa, and annual average discharge at Baruria and the annual rate of bank erosion indicates that annual average discharge at Baruria is strongly related to bank erosion ($r^2 = 0.85$, $p = 0.05$). A strong correlation was also found between mean flood discharge at Mawa and bank erosion ($r^2 = 0.92$, $p = 0.01$); however, the relation between annual erosion rate and peak flow appears to be non-linear but insignificant ($r^2 = 0.90$, $p = 0.24$).

Analysis of the maximum annual flow on the Padma at Mawa station shows that the river experienced 33 floods in the 50 years (1965–2014) for which data are available. The number of flood events for each of the epochs under study is presented in Table 7. It shows that overall flood frequency is 70%, and has been exceeded in 3 out of the 6 epochs studied. Because of incomplete records or unavailable information over the study period, the dataset is somewhat marred.

3.6 Evaluation of accuracy

The interpretation of positional error associated with channel movement revealed that the mean relative area error is ranging from 7 to 12% for the left bank. The corresponding values for the right bank were 7–14%. The result of vertical accuracy in terms of RMSE between 1984 and 2008 indicated that the RMSE was relatively lower for 2008 than for 1984 and 1992 (RMSE for 2008 was 0.30, and 0.35 and 3.39 for 1984 and 1992, respectively).

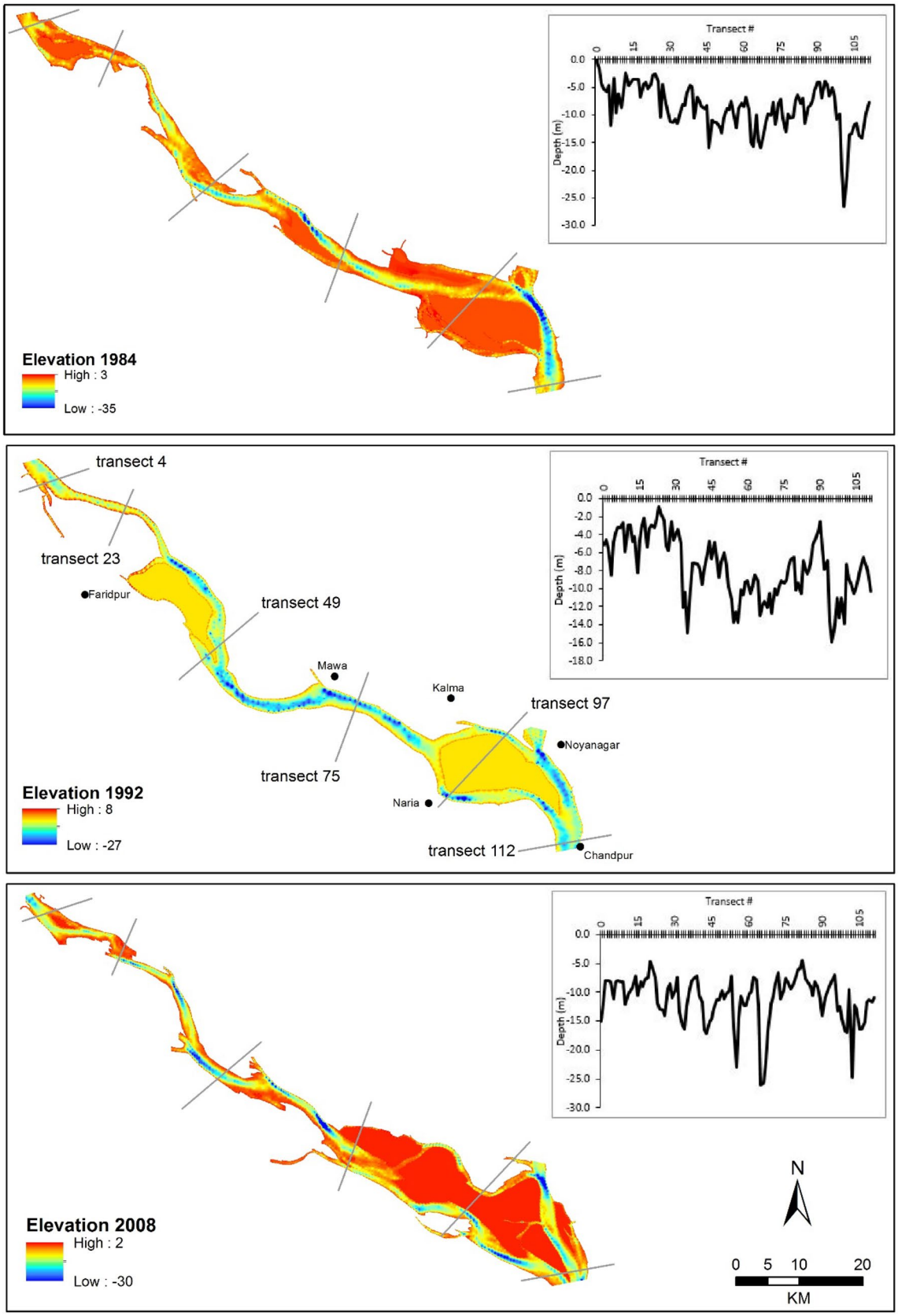

Fig. 4 Riverbed topography and longitudinal profiles of the river Padma in 1984, 1992 and 2008 based on DEMs

Table 4 Quantification of erosion and deposition for the Padma between 1984 and 2008

Before year	After year	Amount fill (m^3)	Amount cut (m^3)	Overall Change[a]	Average change per year (m^3)
1984	1992	673,605,847	334,852,881	338,752,966	42,344,121
1992	2008	465,515,198	760,711,265	− 295,196,067	− 18,449,754

[a]Negative sign indicates volume loss

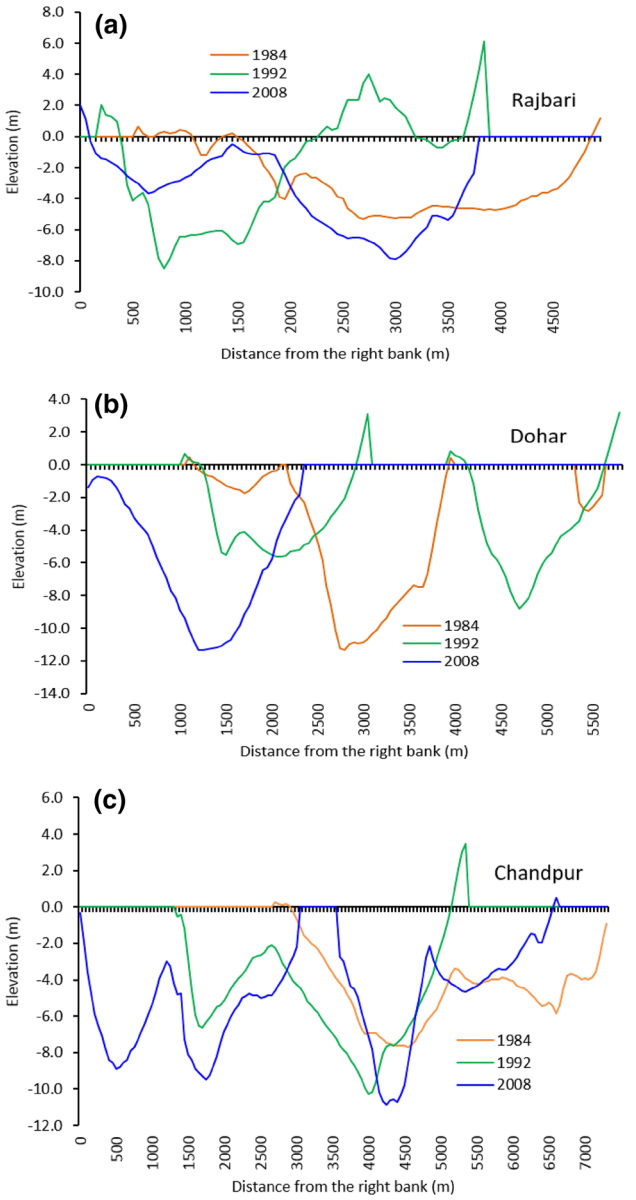

Fig. 5 Representative cross-section changes from 1984 to 2008 derived from DEMs; Cross-section shown from left to right bank: **a** Transect 4 represents the upper reach; **b** Transect 49 covers the middle reach; **c** Transect 112, represents the lower reach. Location of transects is indicated in Fig. 5

4 Discussion

4.1 Planform dynamics

The derived planform evolution illustrates that contraction and expansion of the river varied over time (Fig. 2) which may be attributed to a range of factors, including magnitude and duration of floods (see Fuller 2008; Wallick et al. 2007). Whilst channel narrowing may be related to recovery from flood-induced change (Friedman et al. 1996) and growth of mid-channel bars (Tiegs and Pohl 2005), prolonged and/or intense flooding may enhance channel widths considerably (Rozo et al. 2014; Fuller 2008) due to the capacity of the channel being frequently exceeded (Mount 1995). Consequently, a channel tends to adjust by expanding its cross-sectional area with increasing flood frequency (Winterbottom 2000).

Historical information indicates that the Padma experienced a number of moderate to severe floods during 1910–1922 (Mahalnobis 1927) which may have caused channel expansion in early epochs though we have no data to verify this. Because of many large floods occurring since 1954 in Bangladesh (Mirza 2011), channel widening seems to have been prominent, particularly after 1984 (Fig. 2), which may possibly have been controlled by increasing variations in discharge. Although the role of floods in planform change is debatable (Lewin 1989), it is likely to be one of the major drivers in shaping the Padma's planform. Hickin (1983) indicated that large floods may introduce long periods of channel instability and can lead to a flood-dominated channel morphology, and this observation appears to support our findings. However, more works are required to confirm this. Further, the hydrological cycle of Bangladesh is characterised by a long period (about 8 months) of low flow and a much shorter period of very high discharge (July–October). Hence, inter-annual climatic variations might have influenced observed planform dynamics of the Padma (FAO 2007).

4.2 Pattern of erosion and accretion

Although comparable work is lacking due to differences in methods, the study shows that overall erosion surpassed accretion over the last 100 years (1749 km^2 erosion to

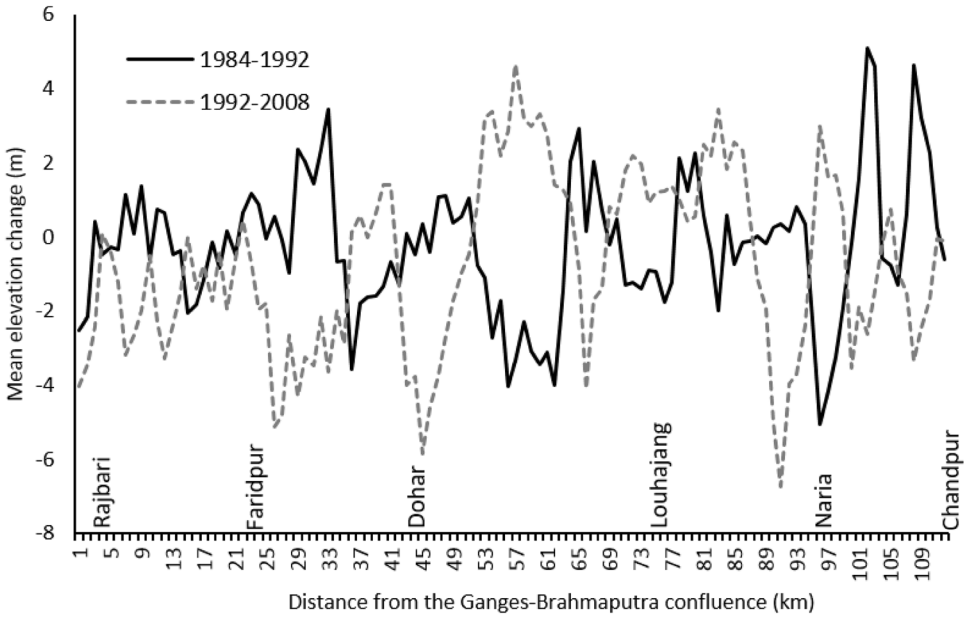

Fig. 6 Mean elevation changes of riverbed between 1984 and 2008

Table 5 Temporal variations in islands area, channel area, mean width and ratio of island area to channel area in the study reach

Year	Channel area (km^2)	Islands area (km^2)	Mean width (km)	Ratio of island area to channel area
1911	193	349	4.9	0.6
1930	307	433	6.8	0.7
1944	297	691	8.9	0.4
1955	282	663	8.6	0.4
1967	381	457	7.9	0.8
1977	279	420	7.0	0.7
1984	323	411	7.1	0.8
1995	459	404	8.4	1.1
2005	545	415	9.3	1.3
2015	559	415	9.2	1.3

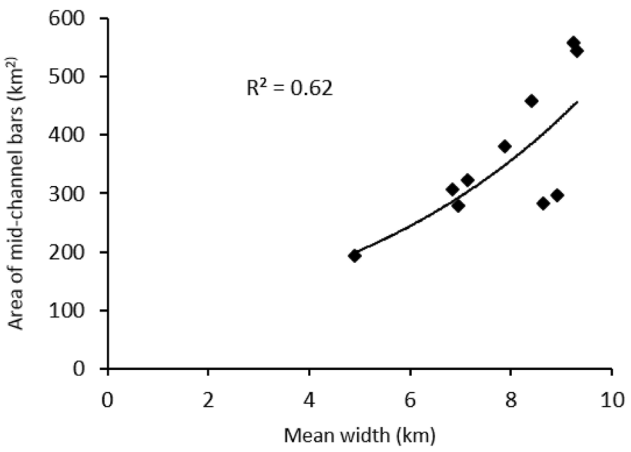

Fig. 7 Relationship between mean channel width and area of mid channel bars, 1911–2015

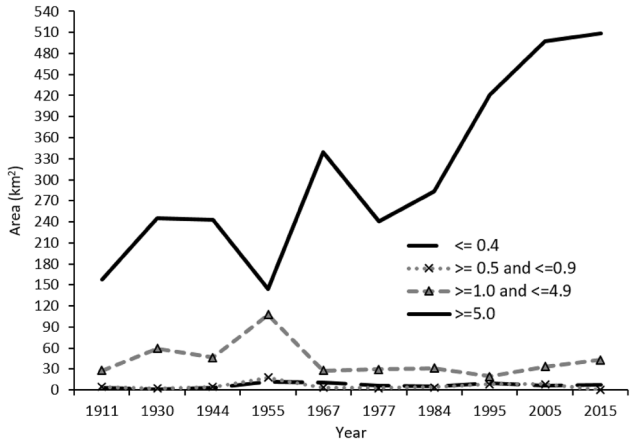

Fig. 8 Areas of mid-channel bars over time, 1911–2015

Table 6 Mean flood discharge at Mawa versus annual rate of bank erosion and accretion, 1967–2015

Epoch	Mean flood discharge (Jul–Oct) at Mawa station	Erosion rate (km^2 $year^{-1}$)	Accretion rate (km^2 $year^{-1}$)
1967–1977	74,159	10	24
1977–1984	68,268	17	12
1984–1995	79,440	18	6
1995–2005	76,790	21	11
2005–2015	66,305	14	13

1316 km^2 accretion = 433 km^2 loss of land) (Tables 2, 3). This finding generally agrees with other works conducted on the same river (see Rahman and Alam 1980; FAP 16 1995; Nippon Koei Co. Ltd. 2005) but differs in magnitude.

Table 7 Flood frequencies for the Padma (floods were categorised as being discharges greater 79,500 m^3/s at Mawa gauging station)

Epoch	Number of floods	Frequency (%)
1965–1967	2	100.0
1967–1977	6	66.7
1977–1984	2	28.6
1984–1995	9	81.8
1995–2005	8	80.0
2005–2014	6	60.0
Total	33	69.5

Compared with large alluvial systems such as the Yellow and the Upper Amazon (Rozo et al. 2014), the magnitude of erosion and deposition of the Padma is not negligible. For example, Yao et al. (2011) observed a maximum erosion rate of 27 km^2 $year^{-1}$, compared with an accretion rate of 18 km^2 $year^{-1}$ for the Yellow River, but we obtained a maximum erosion rate of 17 km^2 and accretion rate of 13 km^2 $year^{-1}$. Studies have shown that bank erosion is the outcome of long-term channel change, floodplain development and destruction (Couper 2004), channel adjustment in response to changes in environmental conditions (Fuller 2008), sediment redistribution (Croke et al. 2013), modified flow conditions and/or bank resistance (Lane et al. 2003). Although human history is relatively short, increased human–environment interaction, especially in recent years, in concert with frequent large floods may have contributed to bank erosion in the Padma, although understanding the impact of human activities on channel change is beyond the scope of this work. A similar observation has been reported elsewhere (Wallick et al. 2007, Surian 1999).

Apart from overall erosion and deposition pattern observed in the channel, the location and magnitude of erosion and depositional contradicts with previous studies on the Padma for individual banks, perhaps owing to the scale of digitization (1:5000) to capture channel geometry and mid-channel bars. Both Tiegs and Pohl (2005) and Rozo et al. (2014) pointed out that the scale of data capture is an important issue that could seriously affect the estimation of erosion and deposition rate. Nonetheless, bank erosion seems to be confined, largely, to a few locations along the left bank compared to the right bank though a few locations exhibited simultaneous increase/decrease of erosion and accretion. A number of factors may be accountable for such pattern. For instance, the right bank is composed of recently deposited unconsolidated sediments that are made up of fine sand and silt. Additionally, this bank has a lower elevation than its counterpart, which possibly contributes to high rates of both erosion and accretion (Leopold and Wolman 1957). Floodplains along the left bank are few hundreds to several thousand years old, except at the locations of Mawa and Harirampur (Figs. 2, 3b), where the erosion rate is extremely high (Nippon Koei Co. Ltd. 2005). As the composition of bank materials determines the stability of riverbanks, lack of cohesive materials may facilitate bank failure, and this is also observed elsewhere (Li et al. 2007). A hydrodynamic and morphological study indicated that erosion and deposition pattern of the river is largely determined by sediment transport rate which depends on seasonal variation of velocity and tides (Roy et al. 2016). Apart from this, we noticed, during fieldwork, that both banks have various kinds of man-made structures in place, including road-cum-embankments, revetments, guide bunds etc. Since bank protection is detrimental to the channel and constriction increases stress on the riverbed (Yao et al. 2011), existing bank protection possibly greatly influences erosional and accretion patterns in the Padma. Other important factors could be changes in water–sediment ratio (Schumm 1977) or the straightening effect of large floods (Winterbottom 2000). As existing bank protection measures are based on a stationary climate, they may be of little help to save life and property from extreme events resulting from global change (Milly et al. 2008). Fieldwork indicates that local bank failure at various sites on the river is quite common which could be a major source of sediment transfer to the river in addition to materials from the upstream points.

4.3 Bathymetric change

Bathymetric analysis indicated that the thalweg changed markedly between years, due to the influence of erosion and accretion dynamics. For example, both banks experienced significant erosion during 1984–1995 as inferred from Landsat data (Tables 2, 3), and this may be reflected by sediment deposition in the riverbed during 1984–1992 (Fig. 5a–c, Table 4). Also, the river experienced seven floods ($> 79{,}506$ m^3 s^{-1}) in the same period, of which three exceeded discharge of $> 100{,}000$ m^3 s^{-1}. The stability of the right bank, relative to the left bank, may also have affected this bathymetric change, since the right bank experienced considerable erosion from 1984 to 1995 (Table 2), potentially related to non-cohesive bank materials as well as shear stress of waters. While a similar mechanism for channel migration was reported by Coleman (1969), little effect of flooding on elevation of the channel bed in the Eel River, California, USA was documented by Sloan et al. (2001). However, our result is in agreement with FAP 9 (1992) and Nippon Koei Co. Ltd. (2005). Their studies showed that the channel dynamics of the middle and lower reaches of the Padma are controlled by thalweg but this study exhibited that this is a common feature for the Padma (Figs. 4, 5a–c, 6).

Cross-sectional analysis indicated that changes in the thalweg and movement of bottom materials are likely to play

an important role in bank shifting. All these factors contribute to channel adjustments in response to environmental conditions. For example, Li et al. (2007) state that changes in hydrological regime can considerably affect fluvial processes, which may in turn induce floodplain deposition and bed scouring. Fuller (2008) noted that the geomorphic impact of flooding on the channel is spatially discontinuous and dependent on the timing of flow. While erosion occurs during peak flooding, falling stages may lead to riverbed deposition accompanied by migration of the thalweg (Coleman 1969), signifying the contribution of bank erosion to catchment sediment budget. Note that we had no information on sediment distribution during the peaks and recessions of flood events, so that no detailed analysis can be presented here. Hence, the results of the morphological budgeting and its association with thalweg shifting and floods may be inconclusive, given limitation of our data with regard to fluvial dynamics. Nevertheless, the analysis of locations, magnitudes and trends with comparative elevation changes and the indicative geomorphic processes at work are useful to identify zones of instability both at upstream and downstream locations (Milan et al. 2011).

4.4 Impact of floods on bank erosion

Regression analysis showed that mean flood discharge, peak flow at Mawa and annual average discharge at Baruria is strongly correlated with the annual rate of bank erosion which contradicts the study of Nippon Koei Co. Ltd. (2005), who reported that large floods of 1987, 1988 and 1989 had negligible impact on bank erosion of the Padma. Our result suggests a direct relationship between discharge and erosion (e.g. Yao et al. 2011; Fuller 2008). Additionally, floods of large magnitude may trigger disturbance cascades (Nakamura et al. 2000), meaning that one impact can introduce a series of subsequent adjustments (Wallick et al. 2007).

Analysis revealed that the banks of the Padma experienced about 433 km^2 of land loss over the study period (1911–2015), indicating a considerable loss of material from the channel banks. Floods could be one of the major factors affecting this land loss as the river had many floods since 1965. Others (Wallick et al. 2007; Shields et al. 2000) observe the relation between bank migration and floods, suggesting that stream power associated with moderate to large floods have the potential to trigger bank migration. Fuller (2008) observed that localised confinement of flows and enhanced stream powers during large floods can allow a fluvial system to adjust morphologically, which may be the case for the Padma. Although we lack sediment flow data, analysis of flood frequency and water level records may provide some insights. The Padma has experienced 33 floods since 1965 of which 10 events had discharge > 100,000 $m^3 s^{-1}$. Furthermore, daily water level records at Mawa revealed that the river was above the high water stage (DL = 6.10 m) for 22 times in 50 years (1965–2014), and on many occasions, the flood duration was long enough to impact the channel morphology (Mirza, 2011), particularly those occurring in the 1990s and 2000s. It is, therefore, reasonable to assume that prolonged and frequent flooding drives bank erosion in the Padma as a strong correlation was observed between bank erosion and mean flood flow. A number of studies (e.g. Ikeuchi et al. 2015; Yu et al. 2010) have predicted that monsoonal discharge is likely to increase, as a result of increased rainfall under warmer climate, which could enhance runoff and sediment load in the rivers (Zhu et al. 2008). Consequently, erosion could be aggravated, particularly in the Ganges–Brahmaputra systems.

4.5 Changes in mid-channel bars

As observed in this study, the nature of erosion and deposition appears to be associated with channel widths and channel areas, which in turn are related to the growth of islands and to flooding. This has also been observed by others (Joeckel and Henebry 2008; Nanson and Knighton 1996). Analysis of bar growth over time revealed that smaller islands are generally very unstable compared to the larger ones (Fig. 8), a phenomenon common in other systems (Baki and Gan 2012). Further, the dynamic nature of islands and mid-channel bars may also affect areas of erosion and accretion (Goswami et al. 1999) and a careful examination of Table 5 and Fig. 8 supports this observation. The presence of mid-channel bars within a river, for instance, may lead to flow divergence, and as a result, more rapidly rising waters affecting water and sediments dispersal, especially during floods. This factor could yield high erosion rates by concentrating flow towards the banks–this has been observed in the Yellow River study by Li et al. 2007. However, bar dynamics may also be related to sedimentological readjustment (Sinha and Ghosh 2012). Mikhailov and Dotsenko (2007) argue that riverbed sedimentation in the Ganges system helps to offset basin subsidence or to compensate for sea level rise, possibly leading to the rise of mid-channel bars.

4.6 Evaluation of accuracy

The maximum measurement error of bank locations was estimated to be ± 0.5 mm, corresponding to ± 127 m (14%) on the 1:253,440 topographic maps. A 15-m (± 2.5 m) error margin was also obtained between the manually digitised channel boundary of 2015 and field-derived river locations. Since the magnitude of observed channel change is considerably larger than the error values, the results of this study are still useful (Mount and Louis 2003; Gurnell, 1997). In terms of the vertical accuracy of the bottom elevation models, our analysis demonstrated that the RMSE

was lower for 1984 and 1992 than 2008 DEM, highlighting the effect of high-density datasets in estimating volume changes. Apart from density of survey points, topographic variability and interpolation methods are also believed to influence DEM uncertainty (Saksena and Merwade 2015; James et al. 2012; Bennion 2009).

5 Conclusion

This is a comprehensive work involving two- and three-dimensional datasets to quantify erosion and accretion patterns of the Padma, for a period of more than 100 years. The analysis indicated that the planform of the Padma is highly variable, in both space and time, owing to the fact that it drains massive monsoonal discharges. Over the study period, both narrowing and widening of the channel occurred but channel expansion became a regular phenomenon from 1984 onwards, but at a varying rate. Variations in discharge appear to be largely accountable for geomorphic changes to the river. The study reinforces that floods are an active agent in determining channel migration and changes in volume, especially for the Padma. We believe the outcomes of this work will be useful in determining the morphological responses to increased runoff and varying flows, so that future modes of planform change and bank erosion can be estimated. Appropriate strategies can subsequently be developed to protect important river functions and natural resources, which will eventually help to minimise the effect of erosion on properties.

The study is not without limitations. A major limitation in capturing bank lines around mid-channel bars is associated with identifying cultivable lands. Since these bars are generally cultivated during the dry season, we had no method of detecting and including them in the analysis. Another possible uncertainty may be related to volumetric change analysis. Since common surfaces between two DEMs of the riverbed were lacking, we could not estimate errors related to volumetric change. Further work is, therefore, warranted. Finally, possible positional and elevation inaccuracy may have inherited from the use of large-/small-scale maps and navigational charts. Therefore, various spatial resolutions along with differing epoch intervals may have an effect on the calculation of erosion and accretion reported in this work. In spite of these limitations, this work provides up-to-date information on channel morphology together with key locations of erosion along the Padma in Bangladesh. Information on several other factors could have enhanced understanding of the observed erosion patterns such as data on riparian land use change, and the spatial and temporal dynamics of sediment flow.

References

Baki ABM, Gan TY (2012) Riverbank migration and island dynamics of the braided Jamuna River of the Ganges-Brahmaputra basin using multi-temporal Landsat images. Quat Int 263:148–161

Bangladesh Bureau of Statistics (BBS) (2016) Bangladesh disaster-related statistics 2015: climate change and natural disaster perspectives. Ministry of Planning, Dhaka

Bennion D (2009) Statistical and Spatial Analysis of Bathymetric Data for the St. Clair River, 1971–2007 (No. 2009–5044). US Geological Survey, Reston

Bizzi S, Lerner DN (2015) The use of stream power as an indicator of channel sensitivity to erosion and deposition processes. River Res Appl 31:16–27

CDMP (Comprehensive Disaster Management Programme), (2014) Trend and impact analysis of internal displacement due to the impacts of disaster and climate change. Study Report. Ministry of Disaster Management and Relief, Dhaka, p 130

CEGIS (Center for Environment and Geographic Information Services) (2003) Ganges River: morphological evolution and prediction. CEGIS, Dhaka, p 70

Chavez PS (1996) Image-based atmospheric corrections revisited and improved. Photogramm Eng Remote Sens 62:1025–1036

Coleman JM (1969) Brahmaputra River: channel processes and sedimentation. Sediment Geol 3:129–239

Couper PR (2004) Space and time in river bank erosion research: a review. Area 36:387–403

Croke J, Todd P, Thompson C, Watson F, Deham R, Khanal D (2013) The use of multi temporal LiDAR to assess basin-scale erosion and deposition following the catastrophic January 2011 Locker flood, SE Queensland, Australia. Geomorphology 184:111–126

Dewan A, Corner R, Saleem A, Rahman MM, Haider MM, Rahman MR, Sarker MH (2017) Assessing channel changes of the Ganges-Padma system in Bangladesh Landsat and hydrological data. Geomorphology 276:257–279

FAO (Food and Agricultural Organisation), (2007) Climate variability and change: adaptation to drought in Bangladesh: a resource book and training guide. Asian Disaster Preparedness Center and FAO, Rome, p 66

FAP 16 (Flood Action Plan 16) (1995) The dynamic physical and human environment of riverine charlands: Padma, Irrigation Support Project for Asia and the Near East. Flood Plan Coordination Organization (FPCO), Dhaka

FAP 24 (Flood Action Plan 24) (1996) River survey project. Final report no. 7. Ministry of Water Resources, Government of the People's Republic of Bangladesh, Dhaka

FAP 4 (Flood Action Plan 4) (1993) Southwest area water resources management project., vol 3. Ministry of Water Resources, Government of the People's Republic of Bangladesh, Dhaka, p 104

FAP 9 (Flood Action Plan 9) (1992) Meghna river bank protection, vol 2. Ministry of Water Resources, Government of the People's Republic of Bangladesh, Dhaka

Federal Geographic Data Committee (FGDC) (1998) Geospatial positioning accuracy standards part 3: national standard for spatial data accuracy. National Aeronautics and Space Administration, Virginia, NV, USA

Friedman JM, Osterkamp WR, Lewis WM (1996) The role of vegetation bed-level fluctuations in the process of channel narrowing. Geomorphology 14:341–351

Fuller IC (2008) Geomorphic impacts of a 100-year flood: Kiwitea stream, Manawatu catchment, New Zealand. Geomorphology 98:84–95

Goswami U, Sarma JN, Patgiri AD (1999) River channel changes of the Subansiri in Assam, India. Geomorphology 30:227–244

Gurnell AM (1997) Channel change on the river Dee meanders, 1946-1992, from the analysis of air photographs. Regul Rivers 13:13–26

Hickin EJ (1983) River channel changes: retrospect and prospect. In: Collinson JD, Lewin J (eds) Modern and ancient fluvial systems, International Association of Sedimentologists Special Publication, vol 6. Wiley, New York, pp 61–83

Ikeuchi H, Hirabayashi Y, Yamazaki D, Kiguchi M, Koirala S, Nagano T, Kotera A, Kanae S (2015) Modeling complex flow dynamics of fluvial floods exacerbated by sea level rise in the Ganges-Brahmaputra-Meghna delta. Environ Res Lett 10:124011

IWFM (2010) Field based applied research for the stabilization of major rivers in Bangladesh. Institute of Water and Flood Management, BUET, Dhaka

James LA, Hodgson ME, Ghoshal S, Latiolais MM (2012) Geomorphic change detection using historic maps and DEM differencing: the temporal dimension of geospatial analysis. Geomorphology 137:181–198

Joeckel RM, Henebry GM (2008) Channel and island change in the lower Platte River: Eastern Nebraska, USA: 1855–2005. Geomorphology 102:407–418

Lane SN, Westaway RM, Hicks DM (2003) Estimation of erosion and disposition volumes in a large, gravel-bed, braided river using Synoptic remote sensing. Earth Surf Proc Landf 28:249–271

Leopold LB, Wolman MG (1957) River channel patterns: braided, meandering and straight, vol 282. USGS professional survey papers, Reston, pp 39–85

Lewin J (1989) Floods in fluvial geomorphology. In: Bevan KJ, Carling PA (eds) Floods: hydrological, sedimentological and geomorphological implications. John Wiley and Sons, New York, pp 284–295

Li L, Lu X, Chen Z (2007) River channel change during the last 50 years in the middle Yangtze river, the Jianli reach. Geomorphology 85:185–196

Mahalnobis PC (1927) Report on rainfall and floods in North Bengal. Irrigation Department Government of Bengal, Calcutta, p 90

Mikhailov VN, Dotsenko MA (2007) Process of delta formation in the mouth area of the Ganges and Brahmaputra rivers. Water Resour 34:385–400

Milan DJ, Heritage GL, Large ARG, Fuller IC (2011) Filtering spatial error from DEMs: implications for morphological change estimation. Geomorphology 125:160–171

Milly PCD, Betancourt J, Falkenmark M, Hirsch RM, Kundzewicz ZW, Lettenmaier DP, Stouffer RJ (2008) Stationarity is dead: whither water management? Science 319:573–574

Mirza MMQ (2011) Climate change, flooding South Asia and implications. Reg Environ Chang 1:S95–S107

Mount JF (1995) California rivers and stream: conflict between fluvial process and land use. University of California Press, Berkeley, p 359

Mount N, Louis J (2003) Estimation and propagation of error in measurements of river channel movement from aerial imagery. Earth Surf Proc Landf 30:635–643

Nakamura F, Swanson FJ, Wondzell SM (2000) Disturbance regimes of stream and riparian systems a disturbance cascade perspective. Hydrol Process 14:2849–2860

Nanson GC, Knighton AD (1996) Anabranching rivers: their causes, character and classification. Earth Surf Proc Landf 21:217–239

Nippon Koei Co. Ltd. (2005) River studies, the feasibility study of Padma Bridge in the People's Republic of Bangladesh, vol 5. Jamuna Multipurpose Bridge Authority (JMBA), Dhaka, pp A5–A65

Rahman KS, Alam MK (1980) Instability of river Padma from Goalundo to Chandpur. J IEB 8:17–21 **(Institute of Engineers, Bangladesh)**

Roy B, Haider MR, Yunus A (2016) A study in hydrodynamic and morphological behaviour of Padma river using DELFT3D model. In: Proceedings of the 3rd International Conference on Civil Engineering for Sustainable Development, 12–14 Khulna.

Rozo MG, Nogueira ACR, Castro CS (2014) Remote sensing-based analysis of the planform changes in the upper Amazon river over the period 1986-2006. J S Am Earth Sci 51:28–44

Saksena S, Merwade V (2015) Incorporating the effect of DEM resolution and accuracy for improved flood inundation mapping. J Hydrol 530:180–194

Sarker MH, Thorne CR, Aktar MN, Ferdous MR (2014) Morphodynamics of the Brahmaputra-Jamuna River, Bangladesh. Geomorphology 215:45–59

Schumm SA (1977) The fluvial system. John Wiley and Sons, New York

Scorpio V, Rosskopf CM (2016) Channel adjustments in a Mediterranean river over the last 150 years in the context of anthropic and natural controls. Geomorphology 275:90–104

Shields FD Jr, Simon A, Steffen LJ (2000) Reservoir effects on downstream river channel migration. Environ Conserv 27:54–66

Sinha R, Ghosh S (2012) Understanding dynamics of large rivers aided by satellite remote sensing: a case study from lower Ganga plains, India. Geocarto Int 27:207–219

Sloan J, Miller JR, Lancaster N (2001) Response and recovery of the Eel River, California, and its tributaries to floods in 1955, 1964, and 1997. Geomorphology 36:129–154

Surian N (1999) Channel changes due to river regulation: the case of the Piave River, Italy. Earth Surf Proc Landf 24:1135–1151

Thakur PK, Laha C, Aggarwal SP (2012) River bank erosion hazard study of river Ganga, upstream of Farakka barrage using remote sensing and GIS. Nat Hazards 61:967–987

Tiegs SD, Pohl M (2005) Planform channel dynamics of the lower Colorado river: 1976–2000. Geomorphology 69:14–27

Wallick JR, Grant GE, Lancaster ST, Bolte JP, Denlinger RP (2007) Patterns and controls on historical channel change in the Willamette river, Oregon, USA. In: Gupta A (ed) Large rivers: geomorphology and management. John Wiley and Sons, Hoboken, pp 491–516

Wang S, Li L, Ran L, Yan Y (2016) Spatial and temporal variations of channel lateral migration rates in the Inner Mongolian reach of the upper Yellow River. Environ Earth Sci 75:1255

Winterbottom SJ (2000) Medium and short-term channel planform changes on the rivers Tay and Tummel, Scotland. Geomorphology 34:195–208

Yang X, Damen MCJ, van Zuidam RA (1999) Satellite remote sensing and GIS for the analysis of channel migration changes in the active Yellow river delta. China. JAG 1(2):146–157

Yao Z, Ta W, Jia X, Xiao J (2011) Bank erosion and accretion along the Ningxia-Inner Mongolia reaches of the Yellow river from 1958 and 2008. Geomorphology 127:99–106

Yu WH, Alam M, Hassan A, Khan AS, Ruane AC, Rosenzweig C, Major DC, Thurlow J (2010) Climate change risk and food security in Bangladesh. EarthScan, London

Zhu YM, Lu XX, Zhou Y (2008) Sediment flux sensitivity to climate change: a case study in the Longchuanjiang catchment of the upper Yangtze River, China. Glob Planet Chang 60:429–442